

# Orientation of Hyperfine Tensors with Respect to Chemical Bonds. Experimental and ab Initio SCF + CI Study in the Nitroxide Series

R. Brière,\*† T. A. Claxton,†§ Y. Ellinger,† P. Rey,\*† and J. Laugier‡

Contribution from Laboratoires de Chimie, and Laboratoire de Diffraction Neutronique, Département de Recherche Fondamentale, Centre d'Etudes Nucléaires de Grenoble, 85 X, F.38041 Grenoble Cedex, France. Received December 24, 1980

**Abstract:** The first experimental results are reported for the nitrogen anisotropic hyperfine tensor of a stable nitroxide radical of known geometry, 2,2,7,7-tetramethyl-1,4-diaza-1-oxocycloheptan-5-one ( $A_{xx} = 0.881 \pm 0.005$  mT,  $A_{yy} = 0.680 \pm 0.005$  mT,  $A_{zz} = 3.279 \pm 0.005$  mT); the direction of the  $A_{xx}$  component makes an angle of  $6 \pm 1^\circ$  to the NO internuclear axis.  $H_2NO$ , in planar and nonplanar geometries, has been chosen as a model system to investigate theoretically, using the SCF + CI method, the diversity of ESR spectra of trapped nitroxide radicals. In particular, the variation of the nitrogen isotropic and anisotropic hyperfine coupling constants with geometry has been calculated which correlates well with the few available experimental results.

Nitroxides form one of the most remarkable series of free radicals.<sup>1</sup> Because of their chemical stability, these molecules are increasingly used as important probes in biological,<sup>2</sup> excited-state,<sup>3</sup> and molecular-interaction studies.<sup>4</sup> Contrary to other common functional groups of organic chemistry, the nitroxide group (Figure 1) has no well-defined geometry. It has been found different from one radical to another: X-ray crystallographic studies have shown planar<sup>5</sup> ( $\alpha = 0^\circ$ ) and bent<sup>6</sup> ( $\alpha \neq 0^\circ$ ) geometries. Curiously, little attention has been given to the possible connections between the structural parameters and the observed spectral characteristics of nitroxides in spite of their extensive applications in many fields of physical chemistry.

It seems to be generally assumed in the interpretation of ESR measurements of trapped nitroxide radicals, for example, in proteins or micelles, that the probe is planar, even though experimental structure determinations suggest that nonplanar structures are probable. Since the ESR line shapes observed in spin-label experiments do depend on the anisotropy of the  $g$  and hyperfine tensors and on the relative orientation of their principal axes, it is important to determine how sensitive these observables are to the geometry of the radical.

Very little experimental data exist for the  $\bar{g}$  and hyperfine tensors of nitroxide free radicals,<sup>7,8</sup> and very few ab initio calculations have been reported.<sup>9-12</sup> Although the SCF + CI calculations described here suggest that  $H_2NO$  is a suitable model system for this class of radicals, chemical intuition would prefer  $(CH_3)_2NO$ . The nitrogen isotropic coupling constants  $a_N$  is accurately reproduced<sup>12</sup> as well as the dependence of the coupling on bending at the radical site.<sup>10</sup> Nothing is known, however, about the anisotropic components of the hyperfine tensor.

This paper covers the first experimental determination of the directions of the principal axis of the  $a_N$  hyperfine tensor in a pyramidal stable radical of known geometry:  $\alpha = 20^\circ 6'$  in 2,2,7,7-tetramethyl-1,4-diaza-1-oxocycloheptan-5-one<sup>6c</sup> (**1**) (Figure 2). We report also the first ab initio SCF + CI calculation of the same property as a function of bending for the  $H_2NO$  model compound.

## Experimental Determination

The common technique to determine hyperfine tensors is to take a crystallographically known host crystal where the radical under consideration occupies a substitutional site. To satisfy this condition optimally, we have developed monocrystals of the parent amine **2** (Figure 2). The crystal structure<sup>6c</sup> is monoclinic ( $P2_1/c$ ) with two magnetically inequivalent sites a and b; the two molecules in those positions are in flattened

chair conformations with, fortunately, the  $C_2N_1C_7$  planes almost perpendicular to each other. Then, large monocrystals of amine **2** doped with 1% of nitroxide **1** have been grown from a benzene solution. We assume that the  $C_2N_1C_7$  plane of the nitroxide in the substitutional site coincides with the  $C_2N_1C_7$  plane of the amine which has been replaced. All interatomic distances in the crystal are compatible with this assumption and all intermolecular distances are larger than the sum of the van der Waals radii.<sup>13</sup>

Owing to one-to-one substitution in the unit cell, one has two magnetically inequivalent sites for the nitroxides. This particular property makes it possible to determine the three components of the  $a_N$  tensor in a single experiment. Since the  $C_2N_1C_7$  planes are perpendicular for the radicals trapped in these two sites, rotation of the magnetic field in the  $x^a N_1^a z^a$  plane of nitroxide a automatically covers the  $N_1^b y^b$  axis of nitroxide b (Figure 3).

Typical ESR spectra, observed for the two perpendicular directions of the external magnetic field, are shown in Figure 4. They consist of two superimposed three-lined spectra in agreement with the crystal structure of **2** and support our hypothesis that the incorporated nitroxides occupy two magnetically inequivalent substitutional sites. In addition, the ESR spectrum on Figure 4a shows the so-called "spin-flip" transition<sup>14</sup> due to hyperfine interactions with distant protons in the molecule.

A plot of the nitrogen hyperfine splitting as a function of rotation of

(1) For general reviews, see: (a) Forrester, A. R.; Hay, J. M.; Thomson, R. H. "Organic Chemistry of Stable Free Radicals"; Academic Press: London, 1968. (b) Rassat, A. *Pure Appl. Chem.* 1971, 25, 623.

(2) See, for instance: (a) McConnell, H. M.; McFarland, B. G. *Q. Rev. Biophys.* 1970, 3, 91. (b) Smith, I. C. "Biological Applications of Electron Spin Resonance"; Interscience: New York, 1971. (c) Jost, P.; Waggoner, A. S.; Griffith, O. H. "Structure and Function of Biological Membranes"; Academic Press: New York, 1971.

(3) Green, J. A.; Singer, L. A. *J. Am. Chem. Soc.* 1974, 96, 2730.

(4) (a) Morishima, I.; Ishihara, K.; Tomishima, K.; Inubushi, T.; Yonezawa, T. *J. Am. Chem. Soc.* 1975, 97, 2749. (b) Pilo Veloso, D.; Rassat, A. *J. Chem. Res., Synop.* 1979, 106; *ibid.*, in press.

(5) See, for example: (a) Bordeaux, D.; Lajzerowicz, J. *Acta Crystallogr., Sect. B* 1974, 30, 790. (b) Turley, J. W.; Boer, F. P. *Ibid.* 1972, 28, 1641. (c) Bordeaux, D.; Lajzerowicz, J. *Ibid.* 1974, 30, 2130.

(6) See, for example: (a) Capiomont, A.; Lajzerowicz, J. *Acta Crystallogr., Sect. B* 1974, 30, 2160. (b) Berliner, L. J. *Ibid.* 1970, 26, 1198. (c) Bordeaux, D.; Lajzerowicz, J. *Ibid.* 1977, 33, 1837. (d) Hawley, D. M.; Ferguson, G.; Robertson, J. M. *J. Chem. Soc. B* 1968, 1255. (e) Grand, A.; Rey, P. *Acta Crystallogr., Sect. B* 1979, 35, 2149.

(7) Griffith, O. H.; Cornell, D. W.; McConnell, H. M. *J. Chem. Phys.* 1965, 43, 2909.

(8) Bordeaux, D.; Lajzerowicz-Bonneteau, J.; Briere, R.; Lamaire, H.; Rassat, A. *Org. Magn. Reson.* 1973, 5, 47.

(9) Salotto, A. W.; Burnelle, L. *J. Chem. Phys.* 1970, 53, 333.

(10) Ellinger, Y.; Subra, R.; Rassat, R.; Douady, J.; Berthier, G. *J. Am. Chem. Soc.* 1975, 97, 476.

(11) Davis, T. D.; Christoffersen, R. E.; Maggiora, G. M. *J. Am. Chem. Soc.* 1975, 97, 1347.

(12) Burton, B.; Claxton, T. A.; Ellinger, Y. *Comput. Phys. Commun.* 1979, 17, 27.

(13) Pauling, L. "The Nature of the Chemical Bond"; Cornell University Press: New York, 1960.

(14) Libertini, L. J.; Griffith, O. H. *J. Chem. Phys.* 1970, 53, 1359.

\* Laboratoire Associé au CNRS n° 321.

† Laboratoires de Chimie.

‡ Laboratoire de Diffraction Neutronique.

§ On leave from the Department of Chemistry, University of Leicester, LE 7RH, England.

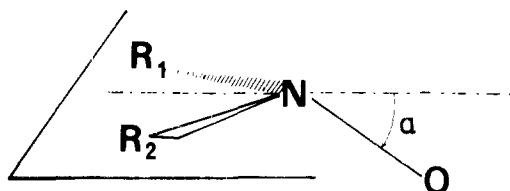


Figure 1. The nitroxide group:  $\alpha$  is the out-of-plane deviation angle.

the magnetic field is given in Figure 5. The parameters of the "best" ellipse, i.e., the directions and magnitude of the principal components of the nitrogen hyperfine tensor, are obtained by a least-squares fit of the experimental curve using the MARQUARDT algorithm. The  $z$  axis is swept after rotation of  $26^\circ$  from the projection of the crystallographic  $0\bar{1}1$  edge on the plane perpendicular to the rotation axis. The  $x$  axis perpendicular to  $z$  is found  $11^\circ$  before the  $0\bar{1}1$  edge projection. The  $y$  axis, determined on the other site, lay at  $38^\circ$  after the  $0\bar{1}1$  edge projection (Figure 3). The principal values of the tensor are:  $A_{xx} = 8.81 \pm 0.05$  G,  $A_{yy} = 6.80 \pm 0.05$  G,  $A_{zz} = 32.79 \pm 0.05$  G. A similar treatment of  $g$  as a function of rotation of the magnetic field shows that the principal axes of the  $\bar{A}$  and  $\bar{g}$  tensors coincide. One obtains:  $g_{xx} = 2.0093 \pm 0.0001$ ,  $g_{yy} = 2.0064 \pm 0.0001$ , and  $g_{zz} = 2.0030 \pm 0.0001$ .

From the structure of the host matrix in which the NO direction is found at  $5^\circ$  from the projection of the crystallographic  $0\bar{1}1$  edge on the plane perpendicular to the axis of rotation, we determine an angle of  $6 \pm 1^\circ$  between the  $x$  axis of the  $\bar{A}_N$  tensor and the NO internuclear axis. This is illustrated in Figure 6 on which is shown a projection of the radical onto the  $xz$  plane of the nitrogen tensor.

The polycrystalline spectrum of 1% of nitroxide in the parent amine gives  $A_{\parallel} = 33.2$  G, which is in good agreement with our experimental value of  $A_{zz}$ . The isotropic  $a_0$  and  $g_0$  values have also been measured for a  $10^{-3}$  M solution of the nitroxide in a liquid amine whose structure is close to that of the host matrix, namely, 2,2,6,6-tetramethyl-4-amino-piperidine. These values are  $a_0 = 15.90 \pm 0.05$  G and  $g_0 = 2.0063 \pm 0.0001$ . They are close to those deduced from single crystal measurements.

$$\frac{1}{3}(A_{xx} + A_{yy} + A_{zz}) = 16.13 \text{ G}$$

$$\frac{1}{3}(g_{xx} + g_{yy} + g_{zz}) = 2.0062$$

The difference between the two series of results reflects the difference between the liquid and the solid states. They confirm our working hypothesis of a one-to-one substitution of the amine with the nitroxide in the host matrix.

#### Theoretical Calculation on the $H_2NO$ Radical

The SCF + CI method is used to calculate the isotropic and anisotropic hyperfine coupling constants as a function of the out-of-plane bending of the radical. All singly excited configurations plus those doubly excited which are responsible for spin-polarization have been taken into account. Although single

Table I.  $a_N$  and  $a_H$  Coupling Constants for Planar  $H_2NO^a$  (gauss)

atom	SCF canonical MO's	SCF $\sigma-\pi$ localized MO's	iterated natural orbitals	type of calcn	
N	iso	0.0	0.0	SCF	
	xx	-1.97	-1.97		
	yy	-3.31	-3.31		
	zz	5.28	5.28		
	iso	5.78	7.84	DPT 1	
	xx	2.62	4.84		
	yy	1.87	4.06		
DPT 2	zz	12.85	14.62		
	iso	8.58	9.00		
	xx	5.31	5.82		
	yy	4.79	5.27		
	zz	15.63	15.91		
	iso	10.70	10.70	12.34	CI
	xx	6.77	6.77	8.21	
CI	yy	6.37	6.37	7.80	
	zz	18.96	18.96	21.01	
	H	iso	0.0	0.0	SCF
		NH	7.02	7.02	
		NH $_{\perp}$	-4.61	-4.61	
		zz	-2.41	-2.41	
		iso	-7.37	-9.15	
NH		1.10	0.78		
NH $_{\perp}$		-12.71	-14.49		
DPT 1	zz	-10.49	-12.17		
	iso	-9.26	-9.07		
	NH	-0.51	-0.40		
	NH $_{\perp}$	-14.70	-14.47		
	zz	-12.57	-12.34		
	iso	-10.36	-10.36	-11.29	CI
	NH	-0.70	-0.70	-1.20	
CI	NH $_{\perp}$	-16.47	-16.47	-17.67	
	zz	-13.91	-13.91	-15.00	

<sup>a</sup> See Figure 7 for visualization of the tensor components. The  $zz$  component can be assigned the  $A_{\parallel}$  experimental values.

determinantal configurations are taken as a basis for the CI expansion rather than spin-adapted configuration state functions, the total wave function is a spin eigenfunction. This is achieved by including all necessary excited determinants.

In a first step, perturbation calculations were also done using the same basis orbitals so that a direct comparison could be made. Standard Epstein-Nesbet double perturbation theory was used in that case.<sup>10,12</sup>

In both CI and perturbation calculations, the hyperfine interactions between an unpaired electron and a magnetic nucleus

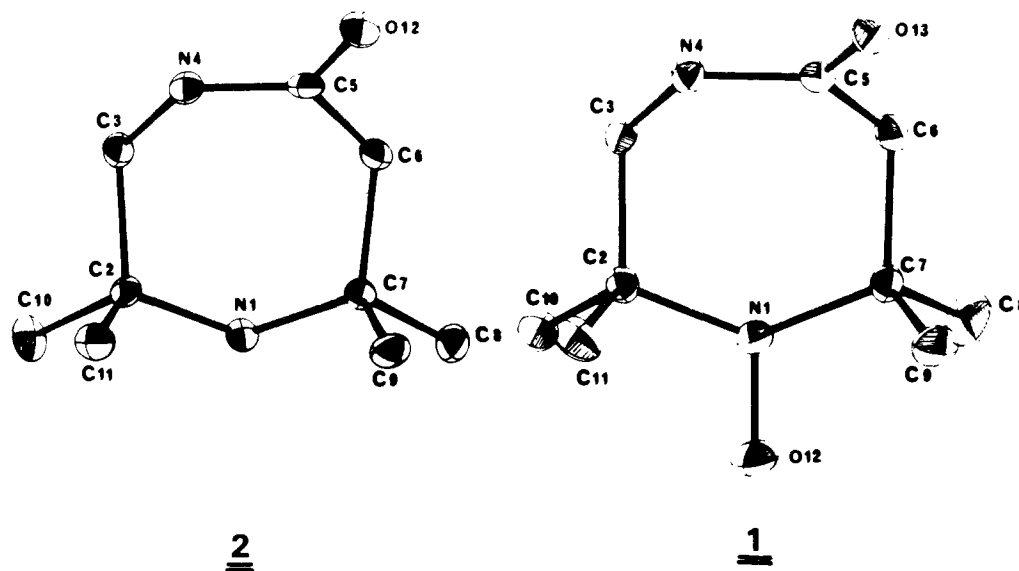
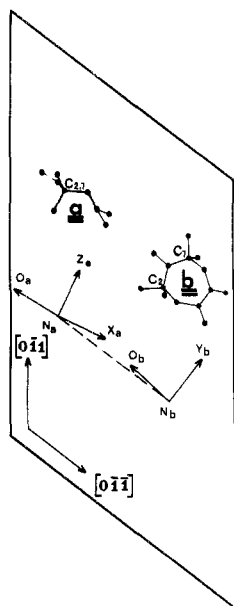
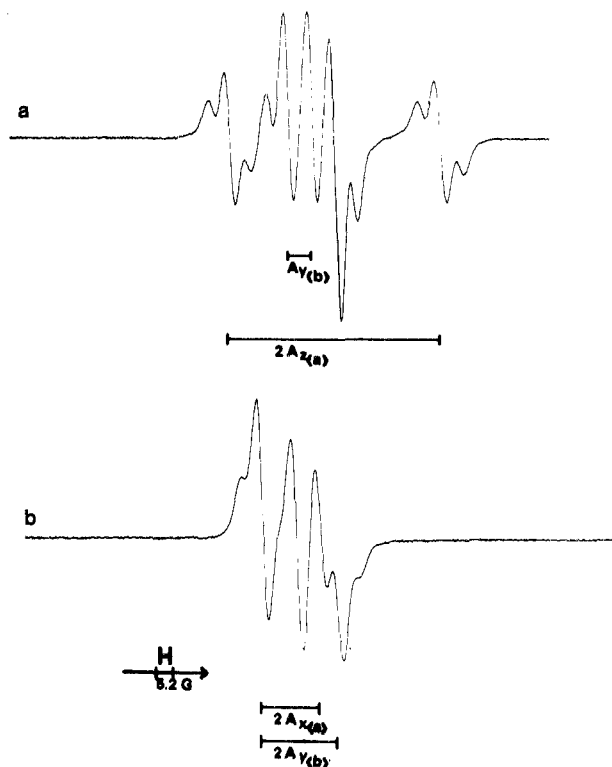


Figure 2. Projection of the nitroxide and parent amine on their average planes showing the numbering of the atoms.



**Figure 3.** Projection of the crystal along the  $C_2C_7$  direction of one of the two magnetically inequivalent sites (site a). Experimental directions  $x_a$ ,  $z_a$  for site a and  $y_b$  for site b are also reported.



**Figure 4.** ESR spectra observed for two characteristic directions of the external magnetic field: (a)  $23^\circ$  after the  $0\bar{1}1$  edge projection; (b)  $113^\circ$  after  $0\bar{1}1$  edge projection (see Figure 4).

$K$  are evaluated as the expectation values of the operators:  $(8\pi/3) g_e \beta_e g_K \beta_K \delta(\vec{r}_K) \vec{S} \cdot \vec{I}$  for the isotropic term, and  $g_e \beta_e g_K \beta_K r^{-3} [3(\vec{L} \cdot \vec{r})(\vec{S} \cdot \vec{r})/r^2 - \vec{I} \cdot \vec{S}]$  for the anisotropic term.

Analytical expressions for the atomic integrals have been given by one of us in a previous paper to which the reader is referred for more details.<sup>15</sup>

The one-particle space in all the calculations described here is obtained by restricted SCF calculations using the McWeeny

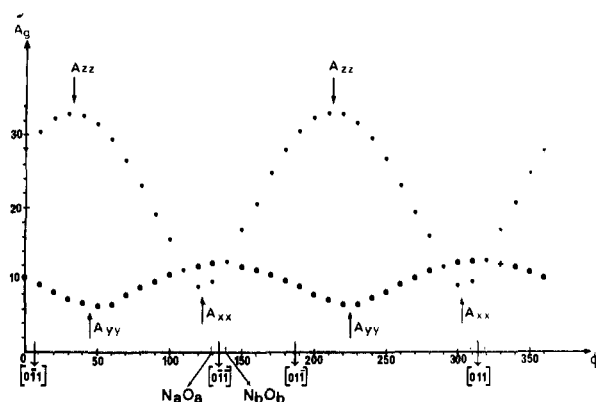


**Figure 5.** Plot of the experimental hyperfine splittings vs. the rotation angle  $\phi$  of the magnetic field. The projections of the NO bonds (sites a and b) and those of crystal edges are shown.

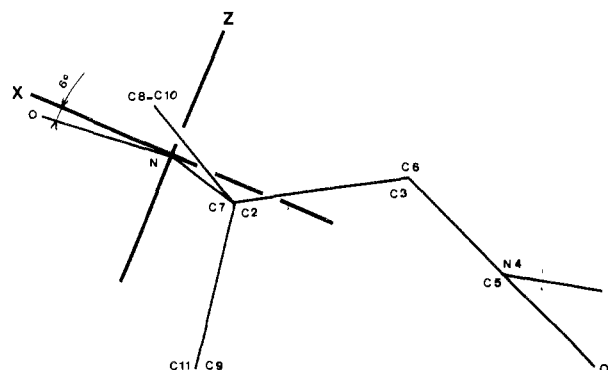


**Figure 6.** Projection of the molecule (site a) along the  $C_2C_7$  direction showing the  $x$  and  $z$  orientation of the hyperfine tensor.

density matrix method.<sup>16</sup> The basis of Gaussian atomic functions is of double  $\zeta$  quality; it is the basis used for a previous study in which the optimized geometry of the  $H_2NO$  radical has been determined.<sup>10</sup>

Experimentally,  $H_2NO$  has been identified in solution<sup>17</sup> with isotropic hyperfine coupling constants  $|a_N| = 11.9$  G and  $|a_H| = 11.9$  G and in solid matrices<sup>18</sup> by the following:  $|A_{\parallel}(N)| = 30$  G,  $|A_{\perp}(N)| = 5-6$  G,  $|a_N| = 13.3-14$  G  $|A_{\parallel}(H)| = 15$  G,  $|A_{\perp}(H)| = 10-11$  G,  $|a_H| = 11.7-12.3$  G

The experimental error is estimated about  $\pm 1$  G for parallel and  $\pm 4$  G for perpendicular features.<sup>18</sup> The oxygen coupling is not known.

## Results and Discussion

Our first calculations of  $H_2NO$ <sup>10</sup> have used first-order double perturbation theory (DPT 1). It was found that separate unitary transformations of the doubly occupied and unoccupied orbital giving localized orbitals (bonding, antibonding, and lone pairs) resulted in different values for the isotropic couplings. Second-order double perturbation theory (DPT 2) greatly improved the calculations for the isotropic couplings and the results closely agreed with the CI results.<sup>12</sup> Illustrative examples of those calculations for the isotropic and our new results for the anisotropic nitrogen and hydrogen couplings are given in Table I for planar  $H_2NO$ .

As can be seen, localization gives a better agreement of DPT 1 calculations with experiment especially for the proton. Although localized orbitals provide also an interpretation of the origins of the hyperfine couplings in terms of chemical bonds,<sup>19</sup> the de-

(16) McWeeny, R.; Sutcliffe, B. T. "Methods of Molecular Quantum Mechanics"; Academic Press: London, 1969.

(17) (a) Adams, J. Q.; Nicksic, S. W.; Thomas, J. R. *J. Am. Chem. Soc.* **1966**, *45*, 654. (b) Gutch, C. J. W.; Waters, W. A. *J. Chem. Soc. A* **1965**, 751.

(18) Mishra, S. P.; Symons, M. C. R. *J. Chem. Res.* (5) **1977**, 174, (M), **1977**, 2075.

(15) Claxton, T. A.; Smith, N. A., *J. Chem. Soc., Faraday Trans. 2*, **1971**, *67*, 1859.

Table II.  $a_N$  and  $a_H$  Coupling Constants as a Function of Bending

$\alpha$ , deg		CI		iterated natural orbitals	
		$a_N$	$a_H$	$a_N$	$a_H$
0	iso	10.70	-10.36	12.34	-11.29
		6.77 <sup>a</sup>	-0.70 <sup>b</sup>	8.21 <sup>a</sup>	-1.20 <sup>b</sup>
10	aniso	6.37	-16.47	7.80	-17.67
		18.96	-13.91	21.01	-15.00
20	iso	11.02	-9.70	12.64	-10.61
		7.14	-0.10	8.56	-0.59
30	aniso	6.74	-15.73	8.15	-16.90
		19.19	-13.26	21.20	-14.32
45	iso	11.87	-7.83	13.44	-8.66
		8.12	1.57	9.51	1.13
60	aniso	7.74	-13.64	9.10	-14.71
		19.76	-11.43	21.71	-12.40
75	iso	12.95	-5.09	14.47	-5.82
		9.39	4.04	10.74	3.66
90	aniso	9.02	-10.57	10.36	-11.52
		20.43	-8.74	22.30	-9.61
105	iso	14.29	-0.27	15.65	-0.81
		11.08	8.42	12.29	8.17
120	aniso	10.75	-5.19	11.94	-5.90
		21.03	-4.06	22.70	-4.71
135	iso	14.76	4.26	15.92	3.90
		11.87	12.67	12.91	12.52
150	aniso	11.59	-0.29	12.61	-0.78
		20.83	0.40	22.24	-0.04

<sup>a</sup> See Figure 7 for visualization of the tensor components. For nitrogen the upper entry corresponds to the  $xx$  direction and the lower entry to the  $yy$  direction. <sup>b</sup> For hydrogen the upper entry corresponds to the NH direction of Figure 7 and the lower entry to the  $NH_{\perp}$  direction.

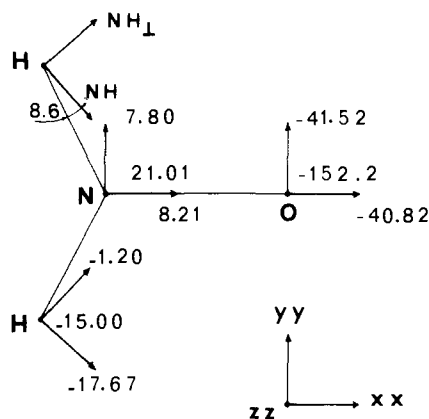


Figure 7. The principal values and axes of the anisotropic components of the hyperfine coupling tensors for planar  $H_2NO$ . All components are in gauss. The numbers close to the nuclei represent components perpendicular to the molecular plane. The arrows point to the values associated with the direction of the axis and do not represent a direction (a tensor component, not a vector component).

pendency of the results on the choice of the orbitals is not satisfactory. In the DPT 2 calculations, much of this dependency is removed, providing a reasonable alternative to CI calculations.<sup>12</sup>

Since correlation effects arising from all doubly excited states (20436 configurations) do not change the results significantly,<sup>12</sup> we limited our treatment of hyperfine interactions as a function of bending to all singly excited plus all spin-polarization configurations. The CI results are reported in Table II together with those obtained by natural orbital iterations. Theoretical anisotropic components of the hyperfine interaction tensors are given in Figure 7 for planar  $H_2NO$  and explain the notation used for designing the various components in Tables I and II.

(19) (a) Ellinger, Y.; Subra, R.; Levy, B.; Millie, P.; Berthier, G. *J. Chem. Phys.* **1975**, *62*, 10. (b) Ellinger, Y.; Levy, B.; Millie, P.; Subra, R. "Localization and Delocalization in Quantum Chemistry"; Chalvet, O. et al., Eds.; D. Reidel: Dordrech-Holland, 1975; Vol. 1, p 283.

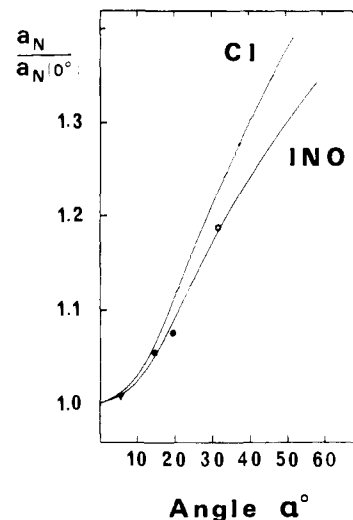


Figure 8. Change in nitrogen isotropic hyperfine coupling constants with geometry of  $H_2NO$ ; CI, configuration interaction; INO, iterated natural orbitals; solid circle, experimental results from known six-membered ring nitroxides (CNC  $\sim 125^\circ$ ); open star within circle, experimental results from known bicyclic nitroxides (CNC  $\sim 116^\circ$ ); solid triangle, experimental results from known five-membered ring nitroxides (CNC  $\sim 112^\circ$ ).

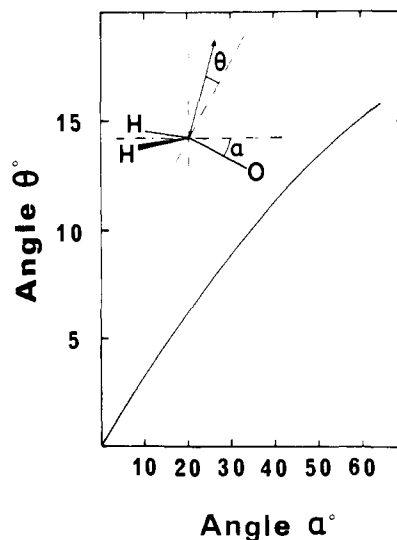


Figure 9. Dependence of the orientation  $\theta$  of the principal component of the nitrogen anisotropic tensor with bending  $\alpha$  of the  $H_2NO$  radical.

Our results are in good agreement with the known experiments on  $H_2NO$  for planar or nearly planar conformations.<sup>20</sup> All isotropic and perpendicular (in the molecular plane) features are well reproduced. For the parallel components, there is a good agreement for hydrogen, but the nitrogen component is too small. Other work<sup>21</sup> has indicated that this will certainly be improved by adding polarization functions to the basis set as we have found in systematic DPT calculations involving one-particle spaces of various sizes and quality.

The suitability of  $H_2NO$  for representing the nitroxide series is well known. This is illustrated here on Figure 8 where we have reported  $a_N(\alpha)/a_N(0^\circ)$  as a function of  $\alpha$  for CI and iterated natural orbital calculations. The experimental points are calculated for radicals with comparable CNC angles for both bent and planar geometries. The results have been taken, in all cases, from

(20) A more comprehensive treatment of  $H_2NO$  including vibrational effects will be presented elsewhere. For example, see: Ellinger, Y.; Pauzat, F.; Barone, V.; Douady, J.; Subra, R. *J. Chem. Phys.* **1980**, *72*, 6390.

(21) Barone, V.; Douady, J.; Ellinger, Y.; Subra, R.; Pauzat, F. *Chem. Phys. Lett.* **1979**, *65*, 542. Ellinger, Y.; Subra, R.; Berthier, G., unpublished material.

EPR experiments in the same solvent for the planar and pyramidal nitroxides.

The dependence of the orientation of the principal component  $A_{\parallel}(\text{N})$  upon bending at the radical site is given in Figure 9. The deviation of the  $A_{\parallel}(\text{N})$  direction from the normal to the NO bond is clearly visible. This is expected since rehybridization at nitrogen certainly occurs when bending increases. It can be remarked that a bending of  $20^\circ$  of the  $\text{H}_2\text{NO}$  model which corresponds to the actual geometry of nitroxide 1 gives a displacement of  $6^\circ$  for  $A_{\parallel}(\text{N})$  equal to that observed in the single-crystal experiment. This numerical agreement is, of course, fortuitous but the overall trend is perfectly reliable. Therefore, it can be expected that the more pyramidal a nitroxide is, the larger the displacement of  $A_{\parallel}(\text{N})$

from the normal direction to the NO bond will be. On another hand, the NH component of the  $a_{\text{H}}$  tensor (Figure 7) is not oriented along the NH internuclear axis. The deviation is about  $9^\circ$ . One must emphasize that such a result is not a particularity of the nitroxide series (see also ref 15) but a general property of the anisotropic tensors when the directions are not determined by symmetry.

Therefore, conclusions as to the geometry of free radicals drawn only from the analysis of the anisotropic coupling tensors with the assumption that chemical bonds have the same direction as one of the tensor components may be largely in error.

Registry No. 1, 41578-59-0;  $\text{H}_2\text{NO}$ , 14332-28-6.

## The Oscillatory Briggs-Rauscher Reaction. 1. Examination of Subsystems<sup>1</sup>

Stanley D. Furrow\*<sup>2a,b</sup> and Richard M. Noyes\*<sup>2a</sup>

Contribution from the Departments of Chemistry, University of Oregon, Eugene, Oregon 97403, and Pennsylvania State University, Berks Campus, Reading, Pennsylvania 19608.

Received February 18, 1981

**Abstract:** In acidic aqueous solution at 25 °C, only slow or nonexistent reaction is observed for any two of the three species iodate ion, hydrogen peroxide, and manganous ion. However, if all three species are present, 0.002 M  $\text{Mn}^{2+}$  catalyzes the iodate oxidation of peroxide at a rate almost 1000 times that in the absence of a catalyst! This remarkable observation, which has already been reported by Cooke, can be explained by postulating that the radical oxidant  $\cdot\text{IO}_2$  is very sluggish at abstracting hydrogen atoms from species like  $\text{H}_2\text{O}_2$  but can oxidize  $\text{Mn}^{2+}$  by electron transfer. A detailed mechanism has been proposed that models semiquantitatively not only the manganous catalyzed iodate oxidation of peroxide but also the simultaneous induced disproportionation of the peroxide and the fact that the concentration of elementary iodine does not increase to a limiting value but rises to a maximum and then decreases toward a small value. Despite this single extremum, the subsystem does not exhibit oscillatory behavior.

The most dramatic oscillating reaction in solution is probably that discovered by Briggs and Rauscher.<sup>3</sup> If appropriate amounts of acidic iodate, hydrogen peroxide, manganous salt, malonic acid, and starch indicator are mixed in aqueous solution, the system repeats several times the sequence colorless  $\rightarrow$  yellow  $\rightarrow$  black  $\rightarrow$  colorless. The frequency is a few times per minute, and the transition from yellow to black is particularly sharp. Shakhshiri<sup>4</sup> has described conditions for an effective demonstration.

If reactants are added at a constant rate to a continuously stirred tank reactor (CSTR), a specific mode of behavior can be maintained indefinitely. De Kepper and others at the University of Bordeaux<sup>5,6</sup> have made especially careful studies of conditions generating different types of behavior such as oscillations and multiple stationary states. They have even identified a single set of flow rates that can generate two different stationary states and one oscillatory state depending upon the previous history of the system!<sup>7</sup>

The investigations in Bordeaux have been primarily phenomenological with little effort to identify the elementary processes responsible for such bizarre behavior. Cooke<sup>8</sup> has recently published an effort to isolate component processes and to develop a

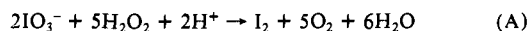
detailed mechanism. Our own studies were carried out independently before we knew of his work. They are reported here in spite of some overlap as noted.

Our efforts to develop an understanding of the mechanism have involved two alternative types of approach. This first paper is concerned with examining various subsystems containing only some of the reactants present in the full system. We have found it particularly informative to examine subsystems containing none of the organic matter present in the full oscillator. The important reactants other than acid are then iodate, hydrogen peroxide, and manganous ion.

The second paper will examine the effects of additions or substitutions of various species. The third paper will attempt to fit all of the information together in order to determine the essential features responsible for the behavior of the full oscillatory system.

### Experimental Observations<sup>9</sup>

**The Iodate-Peroxide Subsystem.** The definitive study of this reaction was by Liebafsky.<sup>10</sup> If product  $\text{I}_2$  is removed rapidly such as by shaking with carbon tetrachloride, the major part of chemical change can be described by stoichiometry A.



Even with his best efforts to remove iodine, Liebafsky<sup>10</sup> observed a stoichiometry that required (A) to be accompanied by some induced disproportionation of hydrogen peroxide according to (B).



(9) Details of procedures are described at the end of the second paper of this series.

(10) Liebafsky, H. A. *J. Am. Chem. Soc.* 1931, 53, 896-911.

(1) Part 40 in the series Chemical Oscillations and Instabilities. Part 39: Noyes, R. M. *J. Am. Chem. Soc.* 1980, 102, 4644-4649.

(2) (a) University of Oregon. (b) Pennsylvania State University.

(3) Briggs, T. S.; Rauscher, W. C. *J. Chem. Educ.* 1973, 50, 496.

(4) Sakashiri, B. Z. "Handbook of Chemical Demonstrations"; University of Wisconsin Press, in press.

(5) De Kepper, P.; Pacault, A. C. R. *Hebd. Acad. Sci., Ser. C* 1978, 286C, 437-441.

(6) Roux, J. C.; Vidal, C. *Nowv. J. Chim.* 1979, 3, 247-253.

(7) De Kepper, P. Dr. es Sci. Thesis, Université de Bordeaux, 1978.

(8) (a) Cooke, D. O. *Inorg. Chim. Acta* 1979, 37, 259-265. (b) *Int. J. Chem. Kinet.* 1980, 12, 683-698.